

Gravity wave modulated airglow observation from spacecraft

S. B. Mende, H. Frey and S. P. Geller

Space Sciences Laboratory, University of California, Berkeley

G. R. Swenson

University of Illinois, Urbana

Abstract. During the STS-75 shuttle mission a special purpose electronic imager viewed the atmosphere below the shuttle orbiter in the wake direction with the objective of imaging gravity wave induced airglow modulation. A continuous sequence of images was taken with a picture repetition rate of 4 per second. A narrow band (3nm) filter was used to select the O₂ atmospheric 0,0 band at 762 nm. The effectiveness of the filter was demonstrated by comparing images of tropospheric clouds with and without filter under full moon conditions. The test showed that the atmospheric O₂ absorption combined with the filter was effective in suppressing intensity variations of the bright full moon illuminated clouds and any other earth albedo. Therefore under conditions of low moonlight the filtered images truly represented the modulation of the airglow intensity uncontaminated by earthshine. Longer sequences of airglow data were processed to compensate for spacecraft motion and to dynamically integrate the signal into a latitude and longitude map of airglow modulations. Because of the intrinsic low pass filtering of the slant view observation geometry preferential enhancement of the higher frequencies was needed to bring out waves in the wavelength range of <200 km. Although the shuttle based limited operation of the imager did not permit to make large area global surveys, the results demonstrated that spacecraft based imaging of the airglow on a long duration flight would produce a global data set much needed for the understanding of Mesosphere Lower Thermosphere dynamics.

Introduction

Atmospheric Gravity Waves are a fundamental factor in the characterization of the energetics and dynamics of the Mesosphere Lower Thermosphere (MLT) region. Waves have a large influence on the MLT region because of their ability to transport significant energy and momentum and to influence larger scale motions. The mean momentum fluxes imply a strong residual circulation near the mesosphere, with upwelling at high summer latitudes and descent in the winter hemisphere which result in temperatures ~90 K above or below radiative equilibrium values and a reversal of the latitudinal gradient of temperature relative to lower altitudes [McIntyre, 1989; Garcia, 1989; Lübken and von Zahn, 1991; Luo et al., 1995]. Although our understanding of gravity waves in the mesosphere has improved considerably in the past decade, quantitative characterization of their role is still in its infancy. Significant advances could be made by a systematic survey of gravity waves which can only be accomplished by spacecraft based imaging.

Copyright 1998 by the American Geophysical Union.

Paper number 97GL03224.
0094-8534/98/97GL-03224\$05.00

Gravity waves can be observed from space by imaging the intensity modulations of the the 80-100 km region. Downward (nadir) viewing from spacecraft would permit the observation of the short wavelength (down to $\lambda_x \sim 10$ km) gravity waves which are most significant in controlling the MLT energy and momentum balance. Slant, not directly downward viewing observations of shorter wavelength gravity waves are limited by line of sight cancellation of closely spaced adjacent intensity maxima of the waves.

There have been numerous investigations centered on ground and space-based optical observations of gravity waves via imaging techniques [see for Taylor, 1997 and references therein].

The primary candidate for spacecraft measurement of gravity wave modulated intense airglow emissions is the O₂ (0,0) band of the $b^1\Sigma_g^+ - X^3\Sigma_g^-$ at 761.9 nm [Tarasick and Shepherd, 1992; Zhang et al., 1993; Hickey et al., 1993]. This band is not visible from the ground because of the deep absorption by the lower atmospheric O₂. Another advantage of the O₂ band is that the high concentration of O₂ in the lower atmosphere absorbs the rescattered emission by the earth. This is a critical advantage in downward viewing observations because the large nonuniformities in the earth albedo could dominate the image modulations. The O₂ absorption of continuum radiation, such as moonlight or man made light sources had not been measured previously in this band.

In this paper we describe observations of airglow intensity modulations observed from the space shuttle. The modulations are attributed to the passage of gravity waves through the airglow layer. In order to image the airglow and resolve the finer scale waves it is necessary to take longer exposures to enhance the SNR and overcome the intrinsic faintness of the airglow, while compensating for the spacecraft motion. We perform such image enhancements data taken on the STS-75 mission with the objective to show feasibility of the technique for long term systematic observation of the airglow and provide the much needed data base for global gravity wave studies.

Observations

The Tether Optical Phenomena (TOP) imager instrument was flown on the STS-75, TSS-1R shuttle mission to observe discharge glows caused by the interaction of the long electrodynamic tether with the atmosphere/ionosphere. The TOP imager was a high sensitivity image intensified CCD camera capable of taking extended exposures. The data discussed in this paper were taken with an interference filter centered at 762 nm with a bandwidth of 3 nm. The imager was mounted inside the orbiter cabin to look through one of the windows to observe the atmosphere below and was shielded from interior light.

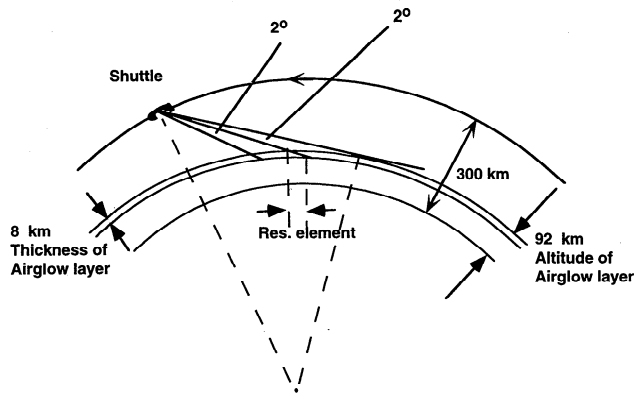


Figure 1. Observation scenario (not to scale). View directions towards the limb tangent and 2 and 4 degrees below that are illustrated.

The observing scenario is illustrated in Figure 1. The shuttle orbiter was in a circular orbit of 300 km altitude and the camera was looking back along the orbit track at the airglow emission layer located ~92 km. The broken lines represent the shuttle position radius vector and the radius vector to the airglow layer tangent point from the center of the earth. At the view direction towards the tangent point the observer is looking parallel to the airglow layer and small scale intensity modulations of the airglow would be averaged due to line of sight cancellation. When the view direction is aimed below the limb tangent (e.g. 2 degrees or below) the structure in the airglow can be resolved with a resolution element defined by the airglow layer thickness (~8km) divided by the tangent of the angle subtended by the view direction and the airglow layer (Van Rhijn angle).

Figure 2 illustrates the effectiveness of the filter and the lower atmosphere to suppress backscattered full moon moonlight from the earth and clouds. The figure shows the comparison between the unfiltered and filtered images. The strong features of moonlit earth limb and clouds (shown in the unfiltered image) are completely suppressed in the filtered image and their intensity is considerably lower than the features of the O_2 airglow. Resonance scattering in the high density lower atmosphere below absorbs all emissions of the same wavelength as the O_2 band components. However for continuum sources such as moonlight considerable leakage would be expected between the absorbing lines of the O_2 band. A code named "MODTRAN" is generally used for the prediction of atmospheric extinction as a function of wavelength and we have run it for the case presented on Figure 2 assuming that the reflecting layers (clouds) are either at 0 km or 8 km altitude. To simulate the geometry we assumed that the instrument was looking 2 degrees and 6 degrees below the direction of the airglow tangent height. By including the elevation of the moon (15 degrees) we obtained a total in band transmission of 7.2% for 0 km cloud elevation at 2 degree view angle and 37% for the 8 km at 6 degree case. Since the observations were taken near full moon, the intensity of the moonlit clouds were about 3 to 5 kR per nm. In the filter band of 3 nm the MODTRAN code predicted a luminosity level ranging from 1 kR to 5 kR with strong intensity dependence on the slant angle. Our test showed that there was no significant (structured) background and no apparent angular dependence of intensity, consequently we believe that the suppression must have been more effective than the model prediction showing that the broadband filter combined with the atmospheric O_2 removes most of the moonlight even in full moon conditions. From this we are reasonably certain that during low moon conditions white light backscatter is not a significant

contaminant of our observations. The wave data presented in this paper were taken during low or moonless conditions.

A typical image of the airglow taken by the TOP camera is shown on Figure 3 essentially upside down with the limb enhanced airglow spanning the image diagonally. Above the bright airglow limb the faint airglow layer is seen. As we gradually look away downward from the tangential view the apparent intensity diminishes towards the top left corner of the image. Superimposed on this apparent gradual intensity variation there are discernible intensity structures showing a few wavelike airglow features almost but not exactly parallel to the enhanced limb.

During the STS-75 mission several sequences of such images were taken over various geographic regions. The repetition rate was 4 images per sec (1/4 sec exposure each). The signal to noise ratio of the images, which was limited by the relatively short exposure, could be greatly improved by co-adding the signal from each volume element while it is in the field of view. As shown in Figure 1, the TOP camera views a 2 degree wide region starting 2 degrees below the limb tangent.

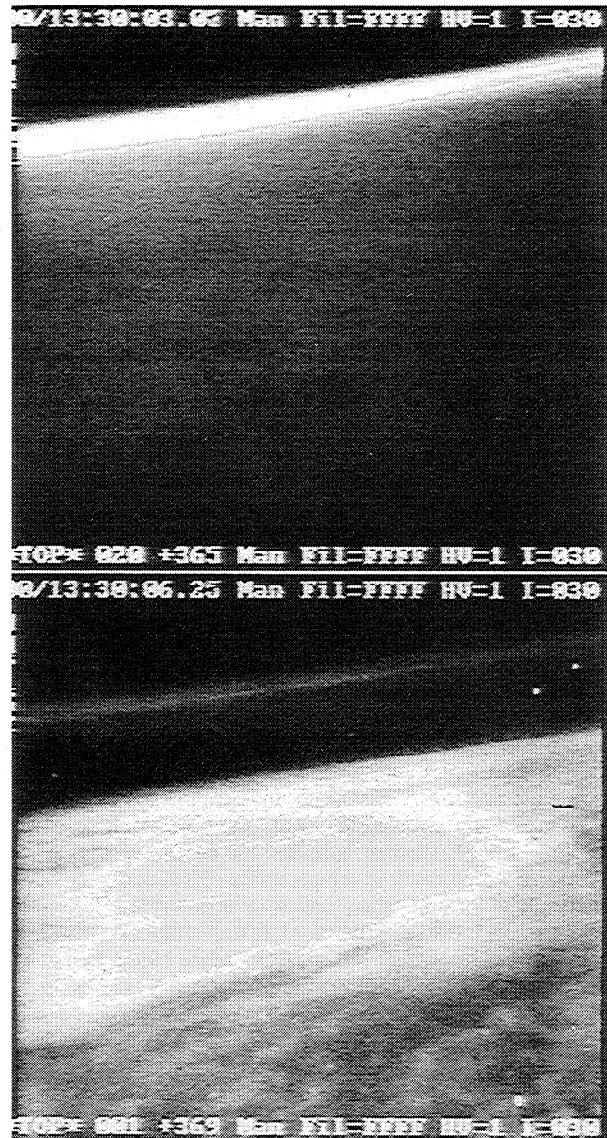


Figure 2. The effectiveness of the filter (combined with O_2 atmosphere) in suppressing white moon-lit earth. Scene with filter, only the airglow is visible (top) filterless scene taken 3 seconds later illuminated by the near full moon (bottom).

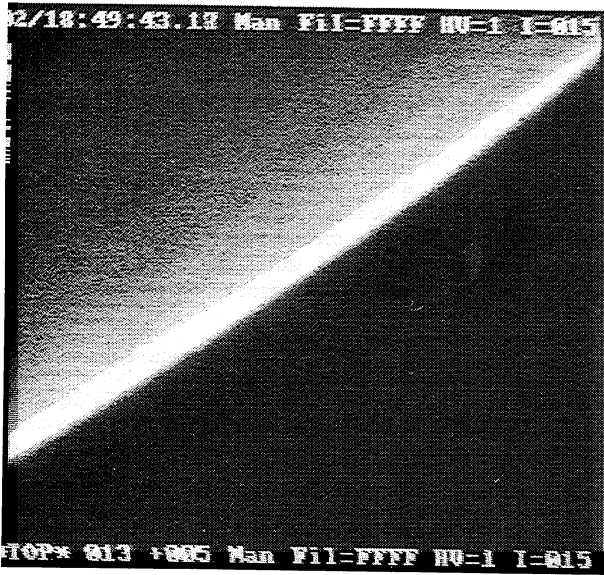


Figure 3. Video frame of the O₂ band airglow layer and wave induced airglow modulations.

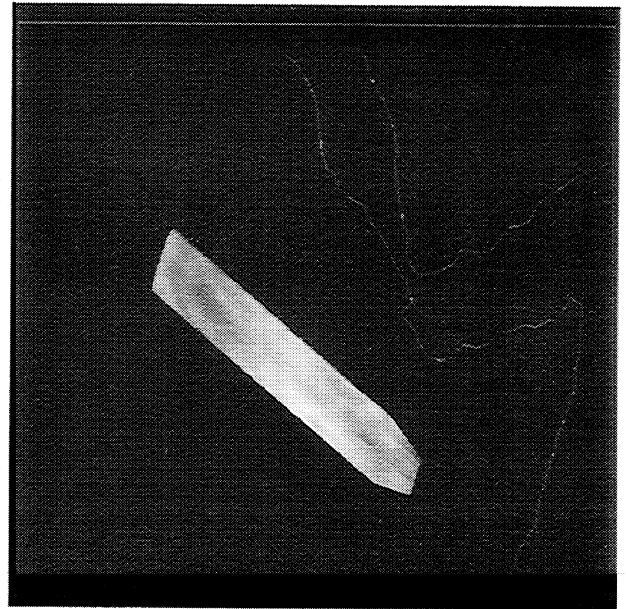


Figure 4. Geographically corrected dynamically integrated data taken between 1507 and 1510 on the 26th of February 1996.

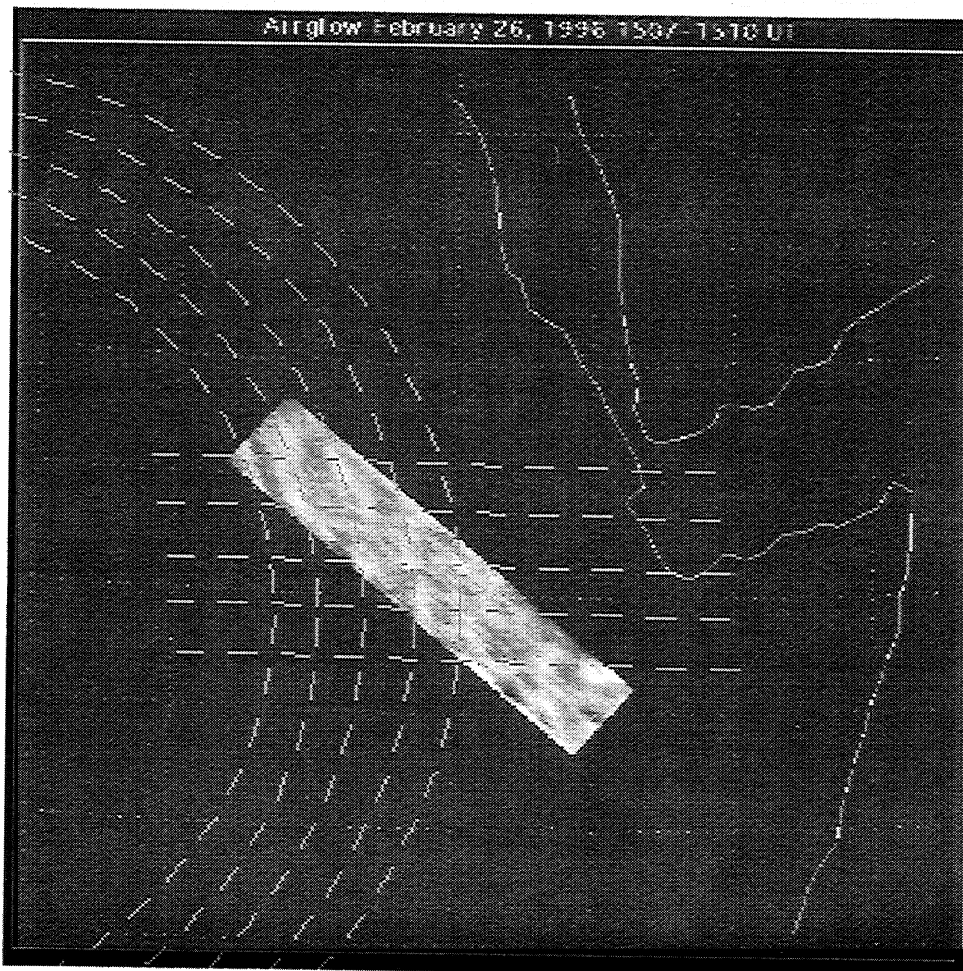


Figure 5. A projection of the Fourier filtered data into geographic coordinates. Broken lines were drawn on the image to illustrate wave patterns which could be consistent with the observed waves.

To perform the intensification, each CCD pixel within this region was projected on a map of resolution elements which were referenced to a geographical grid located on a surface ~90 km above the solid earth. Then as each consecutive exposure was taken the CCD pixels from each exposure were mapped on the same grid taking into account the motion of the shuttle. The signal from each CCD pixel was added to the signal already present at the corresponding resolution element. As the field of view of the CCD moved across a geographic region, the signal was integrated at each geographic resolution element and the signal to noise ratio was thus enhanced. We term this process "dynamical integration".

Discussion

Examination of Figure 4 shows that some of the long wavelength wide area regions have a very high contrast. To enhance the smaller, shorter wavelength, waves selective contrast enhancement was performed by Fourier filtering. The image (Figure 4) was transformed so that the X and Y axes were perpendicular and parallel respectively to the orbit trajectory. The two dimensional Fourier transform of this image was obtained and the very high contrast, low frequency components of the center region of the Fourier transform were blacked out. The resultant transform was inverted and transformed back in its appropriate geographic orientation. This filtering method was tried on several ground based images and it was found that as long as the images do not contain high frequency components from sharp edges or stars the technique does not generate image artifacts. The images described here lack such sharp features and thus they well represent the airglow structure in the selected frequency range. From the transformation of the resultant image into to geographic coordinates (Figure 5) we can see two interfering wave patterns. We have also superimposed the sketch of two wave systems which are consistent with our observations. Recent observations of CO₂ band modulations in the stratosphere show that gravity waves closer to the lower atmospheric source exhibit circular waves pattern propagating from a central origin [Dewan et al., 1997]. Our data is consistent with such a wave propagating mainly in the zonal direction seen in our small observing field and interfering with a weaker wave propagating in the meridional direction.

In ground based zenith observations [e.g Swenson and Mende, 1994] the amplitude of short wave induced airglow intensity modulations is usually of the same order of magnitude as long wavelengths and in fact Hecht et al [1997] show that the slope of the O₂ A band wave number spectrum is -2.42. However, in the STS-75 data, the amplitudes of waves of wavelength 100 km or shorter are so small that they had to be selectively amplified to present them. The need for the enhancement can be explained purely by the geometry of the slant angle, near limb observations. Referring to Figure 1, it can be shown that observing from 2 to 4 degrees below the limb tangent results in line of sight integration spanning ~100 km resolution elements accounting for the need to preferentially amplify the shorter wavelengths.

A shortcoming of the STS-75 data set is the relatively sporadic nature of the airglow data taken during the mission. Nevertheless the STS-75 TOP mission provided several example data sets (one of which was presented in this paper) which demonstrate what can be obtained by an unoptimized slant viewing camera. We have also shown that the O₂ (0,0) band is ideal for topside airglow imaging because of the absorbing qualities of the lower atmosphere in this band. This work can be considered a precursor for performing a future investigation in which long duration continuous synoptic observation of the waves will be made from spacecraft.

Acknowledgments. The authors are greatly indebted to all persons at Lockheed Palo Alto Research Laboratories and at NASA Marshall and Johnson Spaceflight who were involved in the STS-75 flight. The authors acknowledge the contribution of J. L. Mergenthaler and J. B. Kumer of Lockheed-Martin for their contribution in running the MODTRAN code. The work was supported under subcontract No V08971 at Berkeley by the University of Michigan under the SETS NASA contract number NAS8-39381.

References

- Dewan, E. M., et al., MSX: Middle atmospheric Structure in the 4.3 micrometer emission data II; Interpretation in terms of atmospheric gravity waves, AGU Spring meeting 1997.
- Garcia, R. R., Dynamics, radiation, and photochemistry in the mesosphere: implications for the formation of noctilucent clouds J. Geophys. Res., **94**, 14605, 1989.
- Hecht, J. H., R. L. Walterscheid, J. Woithe, L. Campbell, R. A. Vincent, and I. M. Reid, Trends of airglow imager observations near Adelaide, Australia, Geophys. Res. Lett., **24**, 587-590, 1997.
- Hickey, M. P., G. Schubert, R. L. Walterscheid, Gravity Wave-driven fluctuations in the O₂ atmospheric (0-1) nightglow from an extended, dissipative emission region, J. Geophys. Res., **98**, 13,717-13,729, 1993.
- Lubken, F.-J., and U. von Zahn, Thermal structure of the mesopause region at polar latitudes. J. Geophys. Res., **96**, 20841-20857, 1991.
- Luo, Z., D. C. Fritts, R. W. Portmann, and G. E. Thomas, Dynamical and radiative forcing of the summer mesopause circulation and thermal structure. 2. Seasonal variations, J. Geophys. Res., **100**, 3129-3137, 1995.
- McIntyre, M. E., On dynamics and transport near the polar mesopause in summer. J. Geophys. Res., **94**, 14,617, 1989.
- Swenson G. R., S. B. Mende, OH emission and gravity waves (including a breaking wave) in all-sky imagery from Bear Lake, UT., Geophys. Res. Lett., **21**, 2239-2242, 1994.
- Tarasick, D.W., and G.G. Shepherd, Effects of gravity waves on complex airglow chemistries, J Geophys. Res., **97**, 3185-3208, 1992.
- Taylor, M. J., A review of advances in imaging techniques for measuring short period gravity waves in the mesosphere lower thermosphere, Adv. Space Res., **19**, 667-676, 1997.
- Zhang, S. P., R. H. Wiens, and G. G. Shepherd, Gravity waves from O/sub 2/ nightglow during the AIDA 1989 Campaign II: numerical modeling of the emission rate/temperature ratio J. Atmos. Terr. Phys., **55**, 377-395, 1993.
- H. Frey, S. P. Geller, and S. B. Mende, Space Sciences Laboratory, University of California, Berkeley, CA 94720. (e-mail: hfrey@ssl.berkeley.edu, geller@ssl.berkeley.edu, mende@ssl.berkeley.edu)
- G. R. Swenson, Electro-Optic System Laboratory, University of Illinois, 313 Computer and Systems Research Laboratory, 1308 W. Main, Urbana, IL 61801. (e-mail: swenson1@uxl.cso.uiuc.edu)

(Received July 23, 1997; revised October 27, 1997; accepted October 30, 1997.)